Hindawi Publishing Corporation
Journal of Metallurgy
Volume 2012, Article ID 290873, 7 pages
doi:10.1155/2012/290873

Research Article

Effect of Mechanical Milling and Cold Pressing on Co Powder

A. S. Bolokang,[1] M. J. Phasha,[2] D. E. Motaung,[3] and S. Bhero[1]

[1] *Department of Engineering Metallurgy, University of Johannesburg, P.O. Box 17011, Doornfontein 2028, South Africa*
[2] *Council for Scientific and Industrial Research (CSIR), Materials Science and Manufacturing, Meiring Naude Road, Brummeria, P.O. Box 395, Pretoria 0001, South Africa*
[3] *DST/CSIR Nanotechnology Innovation Centre, National Centre for Nano-Structured Materials, Council for Scientific Industrial Research, P.O. Box 395, Pretoria 0001, South Africa*

Correspondence should be addressed to A. S. Bolokang, amogelangblkng6@gmail.com

Received 29 August 2011; Revised 28 October 2011; Accepted 2 November 2011

Academic Editor: Qian Zhao

Cold pressing (CP) of the amorphous-like Co powder suppressed most of the XRD peaks, in particular the peak along (100) plane. The DSC curve of unmilled CP Co powder has shown a distinct sharp exothermic peak at 615°C. Upon annealing at 700°C, only the FCC phase with lattice parameter of 3.51 Å was detected by XRD. Our results implied that the exotherm at 615°C corresponds to compaction-pressure-assisted HCP to FCC first-order phase transition. The XRD analysis of 30 h milled powder revealed for the first time the FCC phase with $a = 3.80$ Å. However, due to presence of (100) and (210) peaks, this phase is thought to be FCT with lattice parameters $a = b = 3.80$ and $c = 3.07$ Å. Consequently, the high-energy milling carried out in the current work induced for the first time HCP to FCT transition in Co. Upon CP of milled powder, the lattice parameter a shrunk from 3.80 to 3.75 Å. However, during annealing of the CP milled Co powder at 750°C, the FCT to FCC transition occurred, yielding the FCC phase with $a = 3.51$ Å.

1. Introduction

Cobalt (Co) is a transition metal used in electronics, magnetic recording [1], and hard materials [2–4]. Through thermal [5] and mechanical treatment [6–9], Co metal undergoes the allotropic HCP to FCC phase transformation. The current literature shows that metastable FCC phase is induced by ball milling (BM) [6], cold pressing [10], and thermal treatments [11]. It has been shown in the previous investigations that Co milled with W, V, and C powders forms the complex FCC Co-rich carbide with large lattice parameters [12]. Apart from the FCC phase, Co-based alloys undergo amorphization via electrodeposition [13, 14] and mechanical alloying (MA) [15–17] and during irradiation processes [18, 19]. It is worth noting that in the case of milling, the XRD peaks of nonmetallic elements such as Si in a mixture with Co vanish rapidly when subjected to BM and ultimately lead to amorphization [17]. Similar behaviour occurs when a mixture of Co and metallic elements is subjected to milling [15, 16, 20]. Amorphous metallic alloys have a promising combination of high magnetic, high strength, and high thermal properties [13]. Amorphization in nonmetallic elements, such as gallium [19], silicon [21], germanium [22], and selenium [23], is easily achievable. However, some studies reported amorphous phases in metallic titanium [24], nickel [25], and cobalt [26, 27] produced via nonequilibrium processing. Among the nonequilibrium techniques, mechanical milling (MM) is a well-known process for producing a wide range of novel materials with unique properties. Of particular interest, MM is capable of forming amorphous alloys [28–31] and composites [32] as well as inducing amorphization in pure elements [23]. On contrary, some amorphous materials were found to undergo the "reverse" process under MM, namely, milling-induced crystallization (MIC) [33–37]. Despite numerous investigations of the phenomenon and mechanisms of MIC, its origin is still surrounded by controversy. The object of the current study to investigate the effects of MM and cold pressing (CP) on the Co powder, and how both processes affect the thermal behaviour.

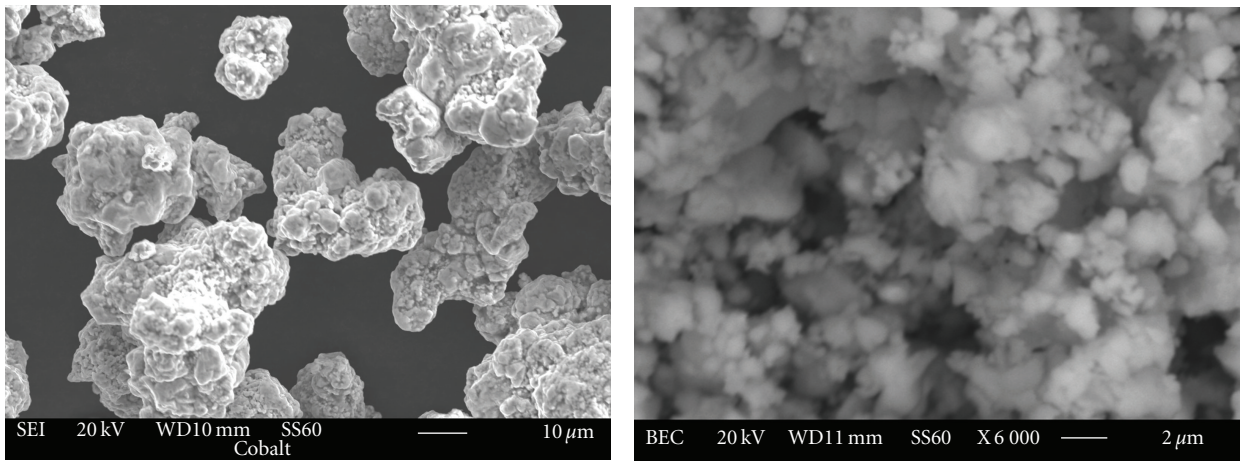

(a) (b)

Figure 1: SEM micrographs of (a) unmilled (b) 30 h milled cobalt powders.

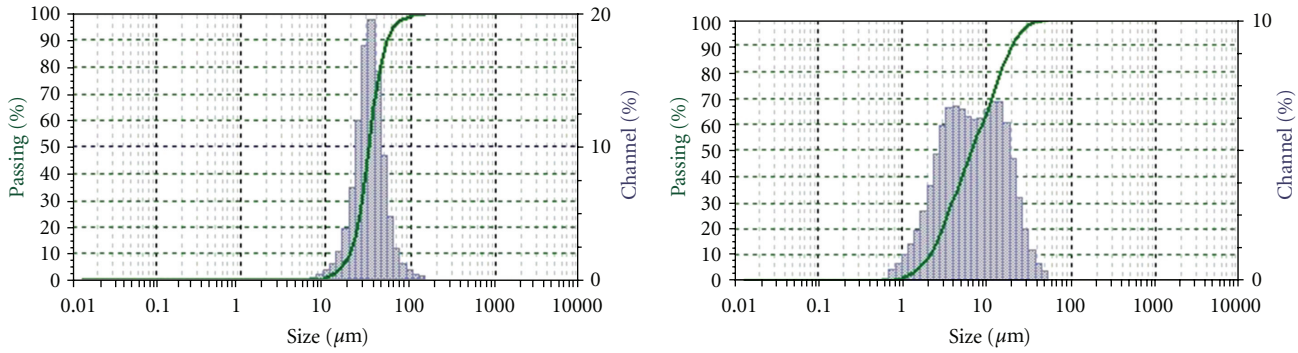

(a) (b)

Figure 2: Particle size distribution in (a) unmilled and (b) 30 h milled Co powders.

2. Experimental Work

In this work, Co powder of 99.8% purity was used. Pure Co powder charge was milled under argon atmosphere at milling speed of 770 rpm for 30 hours (h). Milling was performed in the stainless steel milling medium consisting of 5 mm diameter balls and vial at ball-to-powder ratio of 20 : 1. Milling vial was equipped with cooling system to avoid heating during milling. A small powder sample was used for crystal structure analysis and morphology. The powder morphology was evaluated by LEO 1525 field-emission scanning electron microscope (FE-SEM coupled with a Robinson Backscatter Electron Detector (RBSD) and an Oxford Link Pentafet energy dispersive X-ray spectroscopy (EDX) detector. Phase evolution was traced with a Phillips PW 1830 X-ray diffraction (XRD) machine fitted with Cu Kα radiation, and 0.02 step size scanned from 20° to 90° (2θ). The Microtrac Bluewave particle analyzer was employed to determine the particle size of unmilled and milled Co powders. The thermal analyses of the samples were carried out using a differential scanning calorimetry (DSC) operating at 20°C/min heating rate under argon atmosphere. Annealing was conducted in a tube furnace at heating rate of 20°C/min under argon gas flowing at 20 ml/L standard rate.

3. Results and Discussions

3.1. Powder Characterization. Figure 1(a) shows the SEM micrographs indicating irregular lumps of unmilled Co powder particles. These particles appear to be the agglomerates formed from fine particles. Milling for 30 h fractured these powder lumps into ultrafine particles as displayed in Figure 1(b). In order to validate the particle size reduction, the particle size analyses are presented in Figures 2(a) and 2(b) for unmilled and milled powders, respectively. The unmilled powder is comprised of particles with diameters 19, 32 and 52 μm for cumulative D_{10}, D_{50}, and D_{90}, while particles of diameters 2, 7, and 19 μm constitute the milled powder. Though not presented here, the EDX analysis did not detect any sign of contamination by any of the interstitial elements.

The XRD patterns of the unmilled and cold-pressed Co powders are shown in Figures 3(a) and 3(b), respectively.

Table 1: XRD data of unmilled free, unmilled cold pressed (CP), 30 h milled-free, 30 h milled CP and 30 h milled CP 400°C-annealed Co powder.

Material condition	Space group and number	Phases	Lattice parameter (Å)	
			a	*c*
Unmilled powder	P63/mmc no. 194	HCP	2.51	4.07
Unmilled CP	P63/mmc no. 194	HCP	2.50	4.06
Milled powder	Fm-3m no. 225	FCC	3.80	—
Milled CP	Fm-3m no. 225	FCC	3.75	—
Milled CP annealed	Fm-3m no. 225	FCC	3.80	—

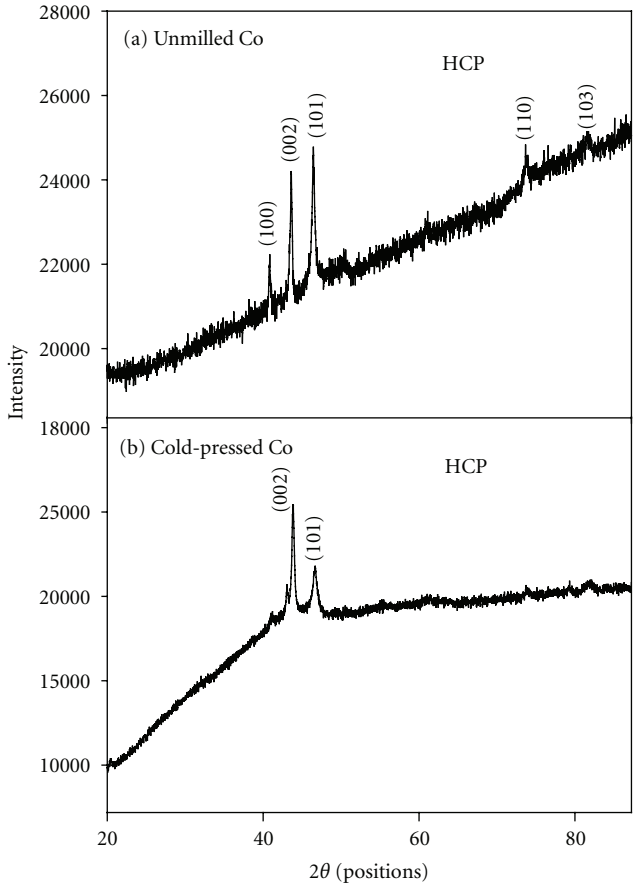

Figure 3: XRD patterns of (a) unmilled and (b) cold-pressed Co powders.

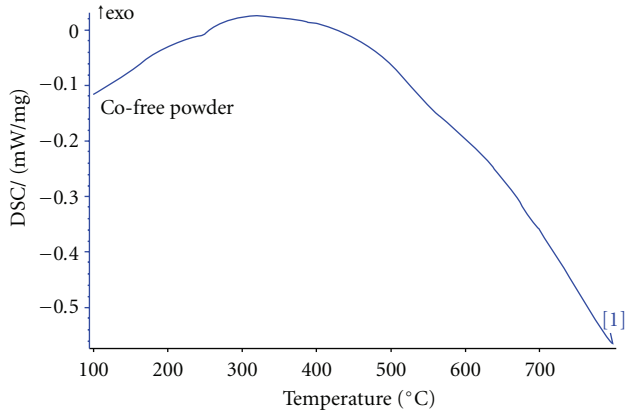

Figure 4: DSC curve of unmilled free Co powder.

Three intense HCP peaks belonging to (100), (002), and (101) planes as well as the two weak peaks along (110) and (103) planes are detected by XRD. The weak XRD peaks are an indication of the nanocrystalline-amorphous nature of the starting Co powder used in the current work. The lattice parameters of HCP unmilled Co powder are listed in Table 1.

As shown in Figure 3(b), the subsequent cold pressing (CP) of the amorphous-like Co powder suppressed most of the XRD peaks observed in Figure 3(a). In addition, the XRD pattern changed from a linear type with approximately constant positive slope to nearly bending behaviour, while the XRD peak along (100) plane almost disappears. This significant decrease in peak intensity along (100), (110), and (103) planes could be indicative of lattice planes that are more affected by cold pressing due to compressive shear stress. Consequently, the *a* and *c* lattice parameters of HCP Co were slightly compressed to 2.50 and 4.06 Å, respectively. Since the axial *c/a* ratio decreased from 1.6258 to 1.6222, it follows that the HCP crystal lattice was compressed more along the *c*-axis via prismatic slip as evidenced by suppressed reflection along the (10-10) plane.

The DSC curve of unmilled free Co powder is presented in Figure 4, showing a very broad exothermic peak above 250°C possibly due to structural relaxation of strain [38] introduced by rapid cooling during atomization process. Unless this strain is released, it will be difficult to observe the HCP to FCC allotropic transition occurring above 420°C. From the DSC curve of unmilled CP Co powder shown in Figure 5, a distinct sharp exothermic peak is observed at 615°C. This figure indicates that the effect of cold pressing is evident upon thermal treatment. The exotherm corresponds to a crystallization process or alternatively because of an annihilation process of pores inside the compacted sample [38–40]. However, it is also possible that the exotherm is an indication of pressure-assisted HCP to FCC martensitic transformation upon heating as opposed to usual thermal-induced transition [41]. In order to clarify this notion, the unmilled powder compact was annealed at 700°C for an hour. As shown in Figure 6, the XRD pattern of the annealed sample has revealed only the FCC phase with lattice parameter of 3.51 Å. This result is attributed to combination

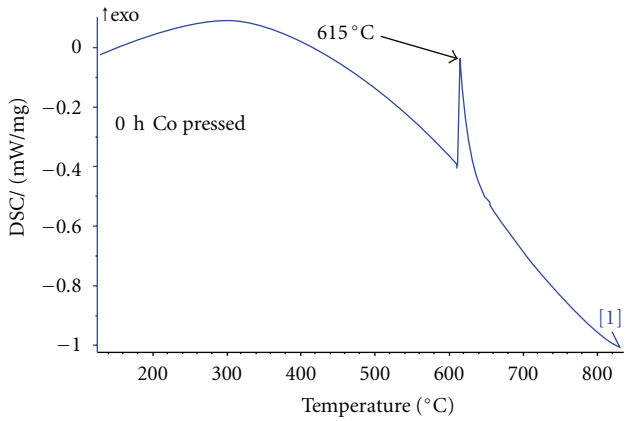

Figure 5: DSC curve of unmilled and cold pressed Co powder.

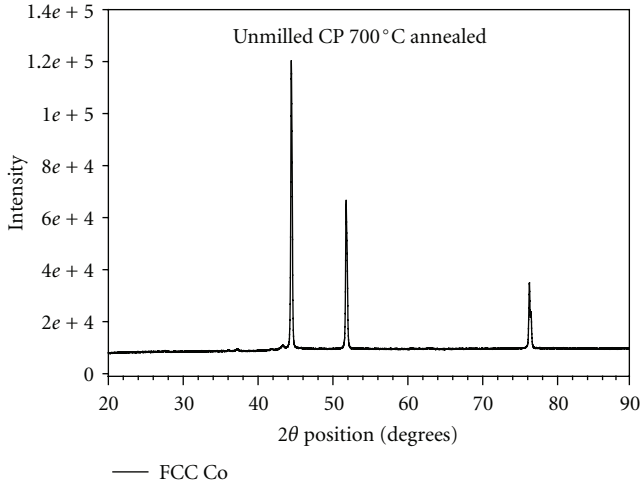

Figure 6: The XRD pattern of the CP sample annealed at 700°C.

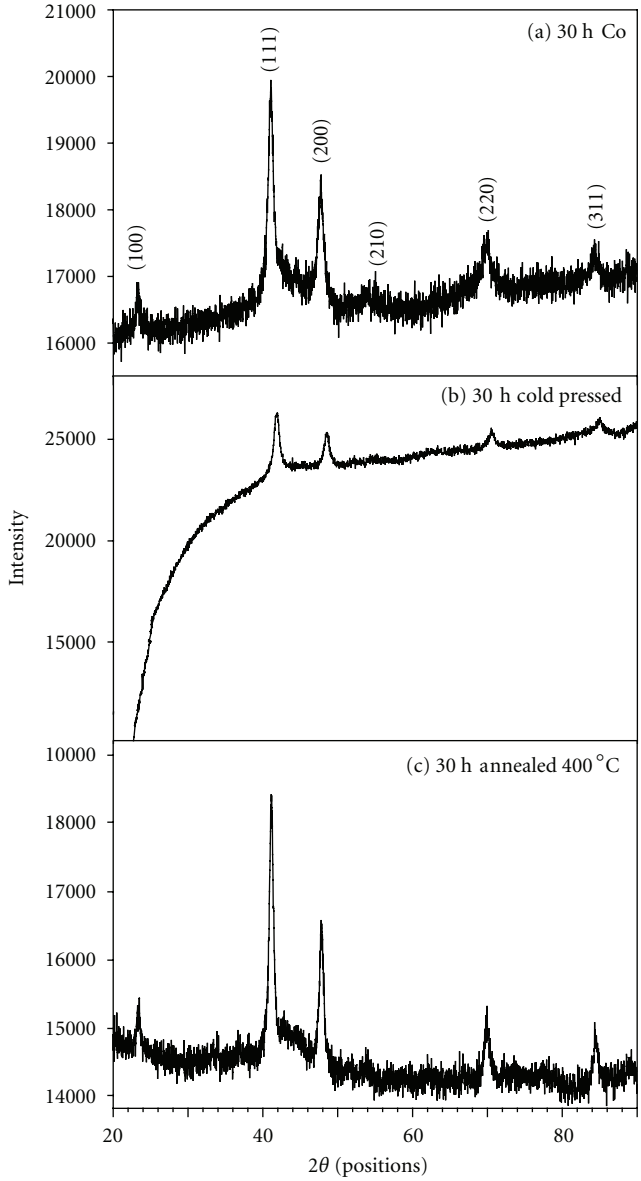

Figure 7: XRD patterns of (a) 30-h milled, (b) cold pressed and (c) 400°C annealed Co powders.

of pressure during CP, the strain in the amorphous-type starting powder, and the heat upon annealing. The resulting FCC phase reveals the exotherm at 615°C as the typical signature for the pressure-assisted first-order phase transition.

Upon extensive 30 h milling, a FCC phase is obtained as shown by the XRD pattern with short and broader peaks in Figure 7(a) due to grain refinement. Although allotropic HCP to FCC phase transformation via MM has been reported before [6–9], the current study finds different results. In addition to the (100) and (210) peaks, the lattice parameter obtained in the current work is 3.80 Å, larger than the previously reported value of 3.54 Å [6]. The larger lattice parameter might imply that the HCP phase actually transformed to FCT (face-centered tetragonal) with lattice parameters $a = b = 3.80$, $c = 3.07$ Å instead of expanded FCC. This possibility would then account for the appearance of (100) and (210) peaks. Using the Scherrer equation, the estimated average crystallite size of the powder was reduced from about 84 nm (before MM) to 45 nm (after MM). Therefore, it should be noted that in current work, the agglomerates of fine-grained powder were used under high milling speed while in previous studies the starting powder was micron sized.

When the milled powder was subjected to cold pressing, the XRD peaks became much shorter and the (100) and (210) peaks disappeared, as shown in Figure 7(b). Similar to what occurred in unmilled HCP Co, the XRD peak of (100) plane in FCC disappeared due to cold pressing. At the same time, the compression of the lattice parameter from 3.80 to 3.75 Å took place upon cold pressing. In order to investigate the thermal behaviour, a DSC analysis was performed on the pressed 30 h milled sample.

The DSC curve in Figure 8 shows endothermic peak around 297°C upon heating the 30 h milled and pressed Co powder, followed by a small and large exothermic peaks at 426 and 707°C, respectively. It is well known that endothermic peaks show phase transformation in certain pure metals

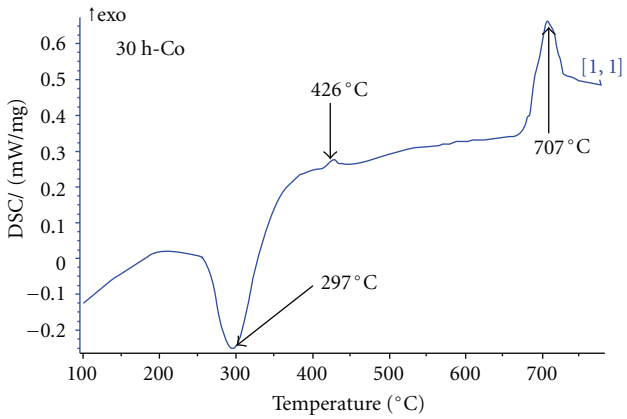

Figure 8: DSC curve of 30 h milled and cold pressed Co.

[42, 43] including Co [5]. However, since our powder has no HCP phase after milling, this endothermic peak at 297°C cannot be related to allotropic HCP to FCC phase transition. To investigate the cause of endothermic peak at 297°C, the pressed sample was annealed at 400°C for 1 hour. It became evident in Figure 7(c) that annealing of the cold-pressed powder changed the XRD pattern to appear similar to that of free flowing milled powder shown in Figure 7(a). It follows that the annealing reversed the cold pressing effect. The (100) plane that was suppressed by cold pressing reappeared, while the lattice parameter also reverted to 3.80 Å. Therefore, it is logical to conclude that the endothermic peak in Figure 8 is a result of washed-out exothermic effect (relaxation of CP mechanical stress), which is a characteristic of many mechanically milled powders [44–46]. On the other hand, the exothermic peaks occurring at 426 and 707°C are due to reordering of the crystallite phase during crystallization process. The difference in temperature might be due to the inhomogeneity of the milling process leading to powder with varying particle sizes as shown in Figure 2(b). However, as was shown for unmilled powder compact, it is possible that the peak at exotherm at 707°C is related to FCT to FCC transition. Consequently, the CP sample was annealed at 750°C, and the corresponding XRD pattern is similar to that in Figure 6. The results therefore validate our hypothesis for possible FCT-FCC transition in milled Co.

Co is an HCP ferromagnetic transition metal placed with FCC metals in the periodic table of elements. It has been shown that Co can either exist as HCP ($a = 2.51$; $c = 4.07$ Å) or FCC with lattice parameter 3.54 Å depending on the grain size [11, 47]. Besides rapid cooling, several authors reported the HCP to FCC phase transformation in Co by MM. Huang et al. [6] showed a close range of variation of FCC Co lattice parameters from 3.53 to 3.56 Å via powder milling. It has been reported that Co can also exist in amorphous structure [26]. The XRD pattern of the cold-pressed sample shows the suppression of the peak belonging to (100) plane, while the lattice parameters become slightly smaller. Our current results support the work of Kirin et al. [10] on effectiveness of cold pressing. They have illustrated phase transformation in Co from FCC to HCP by pressing of the powder. In addition to that, cold pressing can even induce intermetallics reaction [48]. The extensive milling carried out in the current work induced HCP to FCT transition due to mechanical deformation caused by high-speed milling. Several studies illustrated that MM induces crystallization on amorphous materials [49–51]. For example, Bednarčík et al. [50] have milled amorphous CoFeSiB for 800 h to cause crystallization of a mixture of nanocrystalline FCC Co and amorphous phase. An endothermic peak on the DSC curve in Figure 8 corresponds with the volume change of 52.70 mm^3 calculated from the FCC structure after cold pressing from the 55.01 mm^3 obtained after annealing. In our recent work, similar type of endothermic peak accompanied by volume expansion at the Curie temperature of Ni was reported [52]. These types of endothermic peaks that occur in certain pure metals such Ti (HCP to BCC) are assumed to be the resultant of external volume effect, and transformation takes place as a reconstruction of the crystal lattice by both shearing and diffusion process [53].

4. Conclusions

The large lumps of particles in the starting Co powder were fractured into ultrafine particles after 30 h MM, as evidenced by SEM micrographs and particle size distribution analyses. Cold pressing (CP) of the amorphous-like Co powder suppressed most of the XRD peaks, in particular the peak along (100) plane. Since the axial c/a ratio decreased from 1.6258 to 1.6222 due to CP, it follows that the HCP crystal lattice was compressed more along the c-axis via prismatic slip as evidenced by suppressed reflection along the (10-10) plane. The DSC curve of unmilled CP Co powder has shown a distinct sharp exothermic peak at 615°C. Upon annealing at 700°C, only the FCC phase with lattice parameter of 3.51 Å was detected by XRD. Our results implied that the exotherm at 615°C corresponds to compaction pressure-assisted HCP to FCC first-order phase transition. The XRD analysis of 30 h milled powder revealed for the first time the FCC phase with $a = 3.80$ Å. However, due to presence of (100) and (210) peaks, this phase is thought to be FCT with lattice parameters $a = b = 3.80$ and $c = 3.07$ Å. Consequently, the high-energy milling carried out in the current work induced for the first time HCP to FCT transition in Co. Similar to unmilled HCP Co, the XRD peak belonging to the (100) plane of FCT phase disappeared after CP. At the same time, the lattice parameter a shrunk from 3.80 to 3.75 Å due to CP. However, during annealing of the CP milled Co powder at 750°C, the FCT to FCC transition occurred. The lattice parameter of the FCC phase is equal to 3.51 Å.

Acknowledgments

This work was supported by the Department of Science and Technology (DST) of South Africa and the Council for Scientific and Industrial Research (CSIR), Metals and Metals Processing (MMP) Division of the Materials Science and Manufacturing (MSM) Unit.

References

[1] M. P. Pileni, "Mesoscopic domains of cobalt nanocrystals," *Pure and Applied Chemistry*, vol. 74, no. 9, pp. 1707–1718, 2002.

[2] Z. Fang, P. Maheshwari, X. Wang, H. Y. Sohn, A. Griffo, and R. Riley, "An experimental study of the sintering of nanocrystalline WC-Co powders," *International Journal of Refractory Metals and Hard Materials*, vol. 23, no. 4–6, pp. 249–257, 2005.

[3] X. Q. Ou, M. Song, T. T. Shen, D. H. Xiao, and Y. H. He, "Fabrication and mechanical properties of ultrafine grained WC-10Co-0.45Cr3C2-0.25VC alloys," *International Journal of Refractory Metals and Hard Materials*, vol. 29, no. 2, pp. 260–267, 2011.

[4] M. H. Enayati, G. R. Aryanpour, and A. Ebnonnasir, "Production of nanostructured WC-Co powder by ball milling," *International Journal of Refractory Metals and Hard Materials*, vol. 27, no. 1, pp. 159–163, 2009.

[5] H. Matsumoto, "Variation in transformation hysteresis in pure cobalt with transformation cycles," *Journal of Alloys and Compounds*, vol. 223, no. 1, pp. L1–L3, 1995.

[6] J. Y. Huang, Y. K. Wu, H. Q. Ye, and K. Lu, "Allotropic transformation of cobalt induced by ball milling," *Nanostructured Materials*, vol. 6, no. 5–8, pp. 723–726, 1995.

[7] J. Sort, J. Nogués, S. Suriñach, J. S. Muñoz, and M. D. Baró, "Microstructural aspects of the hcp-fcc allotropic phase transformation induced in cobalt by ball milling," *Philosophical Magazine*, vol. 83, no. 4, pp. 439–455, 2003.

[8] J. Sort, J. Nogués, S. Surinach, J. S. Muñoz, and M. D. Baró, "Correlation between stacking fault formation, allotropic phase transformations and magnetic properties of ball-milled cobalt," *Materials Science and Engineering A*, vol. 375–377, no. 1-2, pp. 869–873, 2004.

[9] F. Delogu, "Kinetics of allotropic phase transformation in cobalt powders undergoing mechanical processing," *Scripta Materialia*, vol. 58, no. 2, pp. 126–129, 2008.

[10] A. Kirin, A. Bonefačić, and D. Dužević, "Phase transformation in pressed cobalt powder," *Journal of Physics F*, vol. 14, no. 11, pp. 2781–2786, 1984.

[11] E. A. Owen and D. Madoc Jones, "Effect of grain size on the crystal structure of cobalt," *Proceedings of the Physical Society B*, vol. 67, no. 6, article 302, pp. 456–466, 1954.

[12] A. S. Bolokang, M. J. Phasha, C. Oliphant, and D. Motaung, "XRD analysis and microstructure of milled and sintered V, W, C, and Co powders," *International Journal of Refractory Metals and Hard Materials*, vol. 29, no. 1, pp. 108–111, 2011.

[13] S. S. Grabchikov and A. M. Yaskovich, "Effect of the structure of amorphous electrodeposited Ni-W and Ni-Co-W alloys on their crystallization," *Russian Metallurgy*, vol. 2006, no. 1, pp. 56–60, 2006.

[14] M. A. Sheikholeslam, M. H. Enayati, and K. Raeissi, "Characterization of nanocrystalline and amorphous cobalt-phosphorous electrodeposits," *Materials Letters*, vol. 62, no. 21-22, pp. 3629–3631, 2008.

[15] A. M. Bolarín-Miró, F. S.-D. Jesús, G. Torres-Villaseñor, C. A. Cortés-Escobedo, J. A. Betancourt-Cantera, and J. I. Betancourt-Reyes, "Amorphization of Co-base alloy by mechanical alloying," *Journal of Non-Crystalline Solids*, vol. 357, no. 7, pp. 1705–1709, 2011.

[16] S. Louidi, F. Z. Bentayeb, W. Tebib, J. J. Suñol, A. M. Mercier, and J. M. Grenèche, "Amorphisation of Cr-10Co mixture by mechanical alloying," *Journal of Non-Crystalline Solids*, vol. 356, no. 20–22, pp. 1052–1056, 2010.

[17] G. F. Zhou and H. Bakker, "Atomically disordered nanocrystalline Co_2Si by high-energy ball milling," *Journal of Physics: Condensed Matter*, vol. 6, no. 22, article 004, pp. 4043–4052, 1994.

[18] Y. Limoge and A. Barbu, "Amorphization mechanism in metallic crystalline solids under irradiation," *Physical Review B*, vol. 30, no. 4, pp. 2212–2215, 1984.

[19] M. Holz, P. Ziemann, and W. Buckel, "Direct evidence for amorphization of pure gallium by low-temperature ion irradiation," *Physical Review Letters*, vol. 51, no. 17, pp. 1584–1587, 1983.

[20] M. A. Xueming and J. I. Gang, "Nanostructured WC-Co alloy prepared by mechanical alloying," *Journal of Alloys and Compounds*, vol. 245, no. 1-2, pp. L30–L32, 1996.

[21] S. Takeda and J. Yamasaki, "Amorphization in silicon by electron irradiation," *Physical Review Letters*, vol. 83, no. 2, pp. 320–323, 1999.

[22] G. Patriarche, E. Le Bourhis, M. M. O. Khayyat, and M. M. Chaudhri, "Indentation-induced crystallization and phase transformation of amorphous germanium," *Journal of Applied Physics*, vol. 96, no. 3, pp. 1464–1468, 2004.

[23] G. J. Fan, F. Q. Guo, Z. Q. Hu, M. X. Quan, and K. Lu, "Amorphization of selenium induced by high-energy ball milling," *Physical Review B*, vol. 55, no. 17, pp. 11010–11013, 1997.

[24] Y. Wang, Y. Z. Fang, T. Kikegawa et al., "Amorphouslike diffraction pattern in solid metallic titanium," *Physical Review Letters*, vol. 95, no. 15, Article ID 155501, 2005.

[25] Y. Koltypin, G. Katabi, X. Cao, R. Prozorov, and A. Gedanken, "Sonochemical preparation of amorphous nickel," *Journal of Non-Crystalline Solids*, vol. 201, no. 1-2, pp. 159–162, 1996.

[26] C. Xie, J. Hu, R. Wu, and H. Xia, "Structure transition comparison between the amorphous nanosize particles and coarse-grained polycrystalline of cobalt," *Nanostructured Materials*, vol. 11, no. 8, pp. 1061–1066, 1999.

[27] Y. Song, L. L. Henrys, and W. Yang, "Stable amorphous cobalt nanoparticles formed by an in situ rapidly cooling microfluidic process," *Langmuir*, vol. 25, no. 17, pp. 10209–10217, 2009.

[28] C. C. Koch, O. B. Cavin, C. G. McKamey, and J. O. Scarbrough, "Preparation of "amorphous" $Ni_{60}Nb_{40}$ by mechanical alloying," *Applied Physics Letters*, vol. 43, no. 11, pp. 1017–1019, 1983.

[29] L. Schultz, "Formation of amorphous metals by mechanical alloying," *Materials Science and Engineering*, vol. 97, pp. 15–23, 1988.

[30] J. Eckert, L. Schultz, and K. Urban, "Comparison of solid-state amorphization by mechanical alloying and interdiffusion in NiZr," *Materials Science and Engineering A*, vol. 134, pp. 1389–1393, 1991.

[31] I. Börner and J. Eckert, "Phase formation and properties of mechanically alloyed amorphous $Al_{85}Y_8Ni_5Co_2$," *Scripta Materialia*, vol. 45, no. 2, pp. 237–244, 2001.

[32] J. T. Hsieh, C. K. Lin, J. S. Chen, R. R. Jeng, Y. L. Lin, and P. Y. Lee, "Preparation and thermal stability of mechanically alloyed amorphous Ni-Zr-Ti-Si composites," *Materials Science and Engineering A*, vol. 375–377, no. 1-2, pp. 820–824, 2004.

[33] C. Bansal, B. Fultz, and W. L. Johnson, "Crystallization of FeBSi metallic glass during ball milling," *Nanostructured Materials*, vol. 4, no. 8, pp. 919–925, 1994.

[34] M. L. Trudeau, "Deformation induced crystallization due to instability in amorphous FeZr alloys," *Applied Physics Letters*, vol. 64, no. 26, pp. 3661–3663, 1994.

[35] B. Huang, R. J. Perez, P. J. Crawford, A. A. Sharif, S. R. Nutt, and E. J. Lavernia, "Mechanically induced crystallization of metglas $Fe_{78}B_{13}Si_9$ during cryogenic high energy ball milling," *Nanostructured Materials*, vol. 5, no. 5, pp. 545–553, 1995.

[36] J. Xu and M. Atzmon, "Temperature dependence of deformation-assisted crystallization in amorphous $Fe_{78}B_{13}Si_9$," *Applied Physics Letters*, vol. 73, no. 13, pp. 1805–1807, 1998.

[37] Y. S. Kwon, J. S. Kim, I. V. Povstugar, E. P. Yelsukov, and P. P. Choi, "Role of local heating in crystallization of amorphous alloys under ball milling: an experiment on $Fe_{90}Zr_{10}$," *Physical Review B*, vol. 75, no. 14, Article ID 144112, 2007.

[38] J. J. Suñol, A. González, and J. Saurina, "Thermal analysis of two Fe-X-B (X=Nb, ZrNi) alloys prepared by mechanical alloying," *Journal of Thermal Analysis and Calorimetry*, vol. 72, no. 1, pp. 329–335, 2003.

[39] X. J. Gu, F. Ye, F. Zhou, and K. Lu, "Pressure effect on crystallization of mechanically alloyed amorphous $Al_{85}Fe_{15}$ alloy," *Materials Science and Engineering A*, vol. 278, no. 1-2, pp. 61–65, 2000.

[40] F. Ye and K. Lu, "Pressure effect on crystallization kinetics of an Al-La-Ni amorphous alloy," *Acta Materialia*, vol. 47, no. 8, pp. 2449–2454, 1999.

[41] C. Mangler, C. Gammer, H. P. Karnthaler, and C. Rentenberger, "Structural modifications during heating of bulk nanocrystalline FeAl produced by high-pressure torsion," *Acta Materialia*, vol. 58, no. 17, pp. 5631–5638, 2010.

[42] C. Papandrea and L. Battezzati, "A study of the $\alpha \leftrightarrow \gamma$ transformation in pure iron: rate variations revealed by means of thermal analysis," *Philosophical Magazine*, vol. 87, no. 10, pp. 1601–1618, 2007.

[43] A. K. Rai, S. Raju, B. Jeyaganesh, E. Mohandas, R. Sudha, and V. Ganesan, "Effect of heating and cooling rate on the kinetics of allotropic phase changes in uranium: a differential scanning calorimetry study," *Journal of Nuclear Materials*, vol. 383, no. 3, pp. 215–225, 2009.

[44] J. J. Sunol, A. González, T. Pradell, P. Bruna, M. T. Clavaguera-Mora, and N. Clavaguera, "Thermal and structural changes induced by mechanical alloying in melt-spun Fe-Ni based amorphous alloys," *Materials Science and Engineering A*, vol. 375–377, no. 1-2, pp. 881–887, 2004.

[45] M. T. Clavaguera-Mora, J. J. Suñol, and N. Clavaguera, "Relaxation Kinetics of Mechanically Alloyed Powders. Fe-Ni-Si-P: A Case Study," *Journal of Metastable and Nanocrystalline Materials*, vol. 10, pp. 459–466, 2001.

[46] V. V. Boldyrev and K. Tkáčová, "Mechanochemistry of solids: past, present, and prospects," *Journal of Materials Synthesis and Processing*, vol. 8, no. 3-4, pp. 121–132, 2000.

[47] S. Kajiwara, S. Ohno, K. Honma, and M. Uda, "New crystal structure of pure cobalt formed in ultrafine particles," *Philosophical Magazine Letters*, vol. 55, no. 5, pp. 215–219, 1987.

[48] S. D. De la Torre, K. N. Ishihara, and P. H. Shingu, "Synthesis of SnTe by repeated cold-pressing," *Materials Science and Engineering A*, vol. 266, no. 1-2, pp. 37–43, 1999.

[49] Y. Birol, "Crystallization of a $Fe_{36}Ni_{36}B_{28}$ metallic glass during ball-milling," *Scripta Materialia*, vol. 34, no. 7, pp. 1081–1085, 1996.

[50] J. Bednarčík, J. Kováč, P. Kollár et al., "Crystallization of CoFeSiB metallic glass induced by long-time ball milling," *Journal of Non-Crystalline Solids*, vol. 337, no. 1, pp. 42–47, 2004.

[51] M. Pękała, M. Jachimowicz, V. I. Fadeeva, and H. Matyja, "Phase transformations in Co-B-Si alloys induced by high-energy ball milling," *Journal of Non-Crystalline Solids*, vol. 287, no. 1–3, pp. 360–365, 2001.

[52] A. S. Bolokang and M. J. Phasha, "Thermal analysis on the curie temperature of nanocrystalline Ni produced by ball milling," *Advanced Powder Technology*, vol. 22, no. 4, pp. 518–521, 2011.

[53] W. Szkliniarz and G. Smolka, "Analysis of volume effects of phase transformation in titanium alloys," *Journal of Materials Processing Technology*, vol. 53, no. 1-2, pp. 413–422, 1995.